

patients; therefore, animal experiments would be important to validate the results of this study. Clinical diagnosis of endolymphatic hydrops is based on patients' history, symptoms and various otological tests. However, proof of endolymphatic hydrops in a particular patient is rarely obtained. Besides the animal experiments, the accumulation of follow-up MR-imaging studies using present methods, showing a correlation between the progression of image findings and clinical records, would be necessary to verify the utility of the present method using a 3D inversion-recovery sequence with real reconstruction.

Some invasiveness and relatively long scan time might prevent the wide spread of this method in the clinical

setting, especially in the period of acute vertigo attack of Meniere's disease. Rupture of Reissner's membrane during the attack might cause the contamination of endo- and perilymph fluid, and severely decrease the significance of this method.

In conclusion, by optimizing the inversion time, endolymphatic space, perilymphatic space and surrounding bone or air can be separately visualized on a single image using a 3D inversion-recovery sequence with real reconstruction. This method might open the door for the objective evaluation of endolymphatic space disease in clinical settings.

References

- Zou J, Pyykko I, Bjelke B, Dastidar P, Toppila E (2005) Communication between the perilymphatic scalae and spiral ligament visualized by in vivo MRI. *Audiol Neurootol* 10(3):145–152
- Nakashima T, Naganawa S, Sugiura M, Teranishi M, Sone M, Hayashi H, Nakata S, Katayama N, Ishida IM (2007) Visualization of endolymphatic hydrops in patients with Meniere's disease. *Laryngoscope* 117(3):415–420
- Park HW, Cho MH, Cho ZH (1986) Real-value representation in inversion-recovery NMR imaging by use of a phase-correction method. *Magn Reson Med* 3(1):15–23
- Bandai H, Tsunoda A, Mitsuoka H, Arai H, Sato K, Makita J (2002) Fast inversion recovery magnetic resonance imaging with the real reconstruction method: a diagnostic tool for cerebral gliomas. *Neurol Med Chir (Tokyo)* 42(1):5–10
- Naganawa S, Koshikawa T, Nakamura T, Fukatsu H, Ishigaki T, Aoki I (2003) High-resolution T1-weighted 3D real IR imaging of the temporal bone using triple-dose contrast material. *Eur Radiol* 13(12):2650–2658
- Schuknecht HF, Suzuka Y, Zimmermann C (1990) Delayed endolymphatic hydrops and its relationship to Meniere's disease. *Ann Otol Rhinol Laryngol* 99(11):843–853
- Fujino K, Naito Y, Endo T, Kanemaru S, Hiraumi H, Tsuji J, Ito J (2007) Clinical characteristics of delayed endolymphatic hydrops: long-term results of hearing and efficacy of hyperbaric oxygenation therapy. *Acta Otolaryngol Suppl* 1557:22–25
- Schwaber MK (2002) Transtympanic gentamicin perfusion for the treatment of Meniere's disease. *Otolaryngol Clin North Am* 35(2):287–295
- Haynes DS, O'Malley M, Cohen S, Watford K, Labadie RF (2007) Intratympanic dexamethasone for sudden sensorineural hearing loss after failure of systemic therapy. *Laryngoscope* 117(1):3–15
- Ahn JH, Han MW, Kim JH, Chung JW, Yoon TH (2007) Therapeutic effectiveness over time of intratympanic dexamethasone as salvage treatment of sudden deafness. *Acta Otolaryngol*. 2007 Aug 22; 1-4 [Epub ahead of print] DOI 10.1080/00016480701477602
- De Stefano A, Dispenza F, De Donato G, Caruso A, Taibah A, Sanna M (2007) Intratympanic gentamicin: a 1-day protocol treatment for unilateral Meniere's disease. *Am J Otolaryngol* 28(5):289–293
- Griswold MA, Jakob PM, Heidemann RM, Nittka M, Jellus V, Wang J, Kiefer B, Haase A (2002) Generalized auto-calibrating partially parallel acquisitions (GRAPPA). *Magn Reson Med* 47(6):1202–1210
- Salt AN, Henson MM, Gewalt SL, Keating AW, DeMott JE, Henson OW, Jr (1995) Detection and quantification of endolymphatic hydrops in the guinea pig cochlea by magnetic resonance microscopy. *Hear Res* 88(1-2):79–86
- Shinomori Y, Spack DS, Jones DD, Kimura RS (2001) Volumetric and dimensional analysis of the guinea pig inner ear. *Ann Otol Rhinol Laryngol* 110(1):91–98
- Buckingham RA, Valvassori GE (2001) Inner ear fluid volumes and the resolving power of magnetic resonance imaging: can it differentiate endolymphatic structures? *Ann Otol Rhinol Laryngol* 110(2):113–117
- Niyazov DM, Andrews JC, Strelieff D, Sinha S, Lufkin R (2001) Diagnosis of endolymphatic hydrops in vivo with magnetic resonance imaging. *Otol Neurotol* 22(6):813–817
- Koizuka I, Seo Y, Murakami M, Seo R, Kato I (1997) Micro-magnetic resonance imaging of the inner ear in the guinea pig. *NMR Biomed* 10(1):31–34
- Koizuka I, Seo R, Kubo T, Matsunaga T, Murakami M, Seo Y, Watari H (1995) High-resolution MRI of the human cochlea. *Acta Otolaryngol Suppl* 520(Pt 2):256–257
- Koizuka I, Seo R, Sano M, Matsunaga T, Murakami M, Seo Y, Watari H (1991) High-resolution magnetic resonance imaging of the human temporal bone. *ORL J Otorhinolaryngol Relat Spec* 53(6):357–361
- Ito T, Naganawa S, Fukatsu H, Ishiguchi T, Ishigaki T, Kobayashi M, Kobayashi K, Ichinose N, Miyazaki M, Kassai Y (1999) High-resolution MR images of inner ear internal anatomy using a local gradient coil at 1.5 Tesla: correlation with histological specimen. *Radiat Med* 17(5):343–347
- Naganawa S, Koshikawa T, Fukatsu H, Ishigaki T, Aoki I, Ninomiya A (2002) Fast recovery 3D fast spin-echo MR imaging of the inner ear at 3 T. *AJNR Am J Neuroradiol* 23(2):299–302
- Naganawa S, Komada T, Fukatsu H, Ishigaki T, Takizawa O (2006) Observation of contrast enhancement in the cochlear fluid space of healthy subjects using a 3D-FLAIR sequence at 3 Tesla. *Eur Radiol* 16(3):733–737

TECHNICAL NOTE

S. Naganawa
M. Sugiura
M. Kawamura
H. Fukatsu
M. Sone
T. Nakashima

Imaging of Endolymphatic and Perilymphatic Fluid at 3T After Intratympanic Administration of Gadolinium-Diethylene-Triamine Pentaacetic Acid

SUMMARY: By optimizing the inversion time of a 3D inversion-recovery turbo spin-echo sequence at 3T, we obtained separate images of endolymphatic and perilymphatic space 24 hours after intratympanic administration of gadolinium contrast material. In patients with Ménière disease, endolymphatic hydrops were detected not only in the cochlea but also in the vestibule. Fusion of the 2 types of images visualized the entire fluid space of the labyrinth and the spatial relationship of the 2 spaces.

After intratympanic injection of gadolinium-diethylene-triamine pentaacetic acid (Gd-DTPA) in an animal study, Gd-DTPA was absorbed through the round window membrane and was distributed mainly into the perilymphatic space of the labyrinth.¹ Enlarged endolymphatic space in patients with Ménière disease has been successfully recognized as an area with low signal intensity partly surrounded by high-signal intensity perilymphatic fluid on 3D-fluid-attenuated inversion recovery (FLAIR) images obtained after intratympanic injection of Gd-DTPA.² However, the boundary between the cochlear endolymphatic space and surrounding bone was not clear, as both had low signal intensity on 3D-FLAIR images. To visualize endolymphatic space in the labyrinth as high signal intensity, while maintaining the differentiation from perilymphatic fluid space, we selected an inversion time shorter than that of 3D-FLAIR to suppress the signal intensity of perilymphatic fluid with a higher concentration of Gd-DTPA.

Materials and Methods

Patients

A total of 4 patients (3 with clinically diagnosed Ménière disease and 1 with sudden sensorineural hearing loss, ages 38–69 years; 2 men and 2 women) underwent intratympanic administration of Gd-DTPA bis-methylamide (Gd-DTPA-BMA, Omniscan; Daiichi Pharmaceutical, Tokyo, Japan). These patients were scheduled for intratympanic injection therapy with gentamicin (for the 3 patients with Ménière disease) or with a steroid (for the patient with sudden sensorineural hearing loss). We obtained written informed consent from all patients. The institutional review board of our university hospital approved our study.

Intratympanic Gadolinium Injection

The detailed methods for intratympanic gadolinium injection have been reported previously.² According to the results from this previous study, scan delay after intratympanic gadolinium injection was determined as 24 hours to allow the distribution of gadolinium widely in the perilymphatic space of the labyrinth.

Received June 15, 2007; accepted after revision October 2.

From the Departments of Radiology (S.N., M.K., H.F.) and Otorhinolaryngology (M.S., M.S., T.N.), Nagoya University Graduate School of Medicine, Nagoya, Japan.

Please address correspondence to Shinji Naganawa, MD, Department of Radiology, Nagoya University Graduate School of Medicine, 65 Tsurumai-cho, Showa-ku, Nagoya 466-8550, Japan; e-mail: naganawa@med.nagoya-u.ac.jp

DOI 10.3174/ajnr.A0894

Gd-DTPA-BMA was diluted eightfold with saline (v/v 1:7). We injected the diluted Gd-DTPA-BMA intratympanically through the tympanic membrane using a 23-gauge needle and a 1-mL syringe after the patient was placed in the supine position with their head turned approximately 30° away from the sagittal line toward the healthy ear. The diluted Gd-DTPA-BMA was injected until a backflow of fluid into the external ear was observed through a microscope, resulting in an injected volume of 0.4 to 0.5 mL per patient. After the injection, the patients remained in the supine position for 60 minutes with the head turned approximately 60° away from the sagittal line toward the healthy ear.

MR Imaging

We performed all scans on a 3T MR imaging scanner (Magnetom Trio; Siemens, Erlangen, Germany) using a receive-only 12-channel phased-array coil. T1-weighted 3D-fast low-angle shot (FLASH) and conventional 3D-FLAIR imaging were acquired 24 hours after intratympanic injection of diluted Gd-DTPA-BMA. In addition, T2-weighted 3D-constructive interference in the steady state (CISS) imaging was performed to obtain reference images of labyrinthine fluid-space anatomy.

The parameters for 3D-FLASH were as follows: TR, 4.3 ms; TE, 1.97 ms; flip angle, 10° with radio frequency spoiling; matrix size, 256 × 256; and 96 axial 0.8-mm-thick sections covering the posterior fossa with a 16-cm square FOV. The NEX was 2, giving a total scan time of 2 minutes 51 seconds.

The parameters for 3D-CISS were as follows: TR, 11.42 ms, TE, 5.71 ms; flip angle, 50°; matrix size, 320 × 320; and 48 axial 0.8-mm-thick sections with a 16-cm square FOV. The NEX was 1, and the scan time was 3 minutes 42 seconds.

The parameters for 3D-FLAIR were as follows: TR, 9000 ms; TE, 128 ms; flip angle, 180° (constant) for the turbo spin-echo refocusing echo-train; echo-train length, 23; matrix size, 384 × 384; and 12 axial 2-mm-thick sections covering the labyrinth with a 16-cm square FOV acquired with use of the generalized autocalibrating partially parallel acquisition parallel imaging technique with an acceleration factor of 2.³ The NEX was 1, and the scan time was 14 minutes.

In the first 2 patients, 2D inversion-recovery (IR) turbo spin-echo imaging with TR, TE, and echo-train length identical to those of the 3D-FLAIR protocol was performed with various inversion times (2300, 2100, 1900, 1700, 1500, 1300, 1100, 900, 700, and 500 ms) to determine the null point of perilymphatic fluid containing a low concentration of Gd-DTPA-BMA at 24 hours after intratympanic injection. In both patients, 2D-IR with inversion times of 900 and 1100 ms

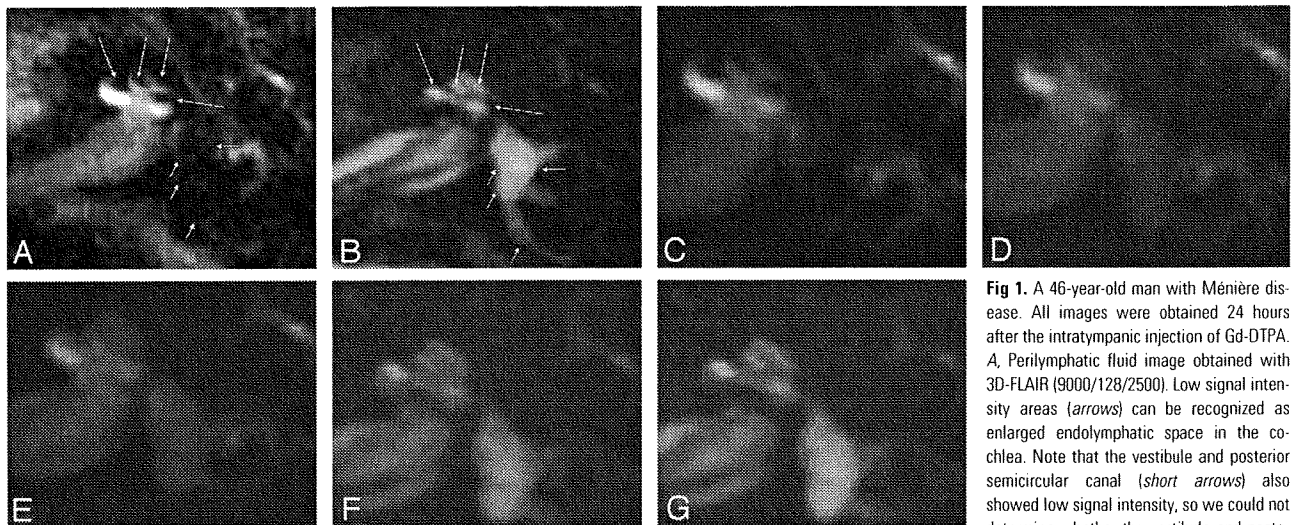


Fig 1. A 46-year-old man with Ménière disease. All images were obtained 24 hours after the intratympanic injection of Gd-DTPA. A, Perilymphatic fluid image obtained with 3D-FLAIR (9000/128/2500). Low signal intensity areas (arrows) can be recognized as enlarged endolymphatic space in the cochlea. Note that the vestibule and posterior semicircular canal (short arrows) also showed low signal intensity, so we could not determine whether the vestibule and posterior semicircular canal were filled with endolymphatic fluid. B, Endolymphatic fluid image obtained with a 3D inversion-recovery sequence (9000/128/1000). Endolymphatic space in the cochlea (arrows) shows high signal intensity on this image. This image confirmed that the vestibule and posterior semicircular canal were filled with fluid. C–G, Fusion of a perilymphatic fluid image (C) and an endolymphatic fluid image (G) with transitional images (D–F). By changing the fusion mixture rate on a workstation, the spatial relationship between perilymphatic and endolymphatic space was easily appreciated in both the cochlea and vestibule. In this case, endolymphatic space was enlarged in both the cochlea and vestibule, but the enlargement was especially prominent in the vestibule. Note that CSF in the internal auditory canal is visualized as high signal intensity on the endolymphatic fluid image (G). The signal intensity of perilymphatic space is just suppressed. Thus, the term *endolymphatic image* is only useful for labyrinthine space.

rrior semicircular canal were filled with endolymphatic fluid. B, Endolymphatic fluid image obtained with a 3D inversion-recovery sequence (9000/128/1000). Endolymphatic space in the cochlea (arrows) shows high signal intensity on this image. This image confirmed that the vestibule and posterior semicircular canal were filled with fluid. C–G, Fusion of a perilymphatic fluid image (C) and an endolymphatic fluid image (G) with transitional images (D–F). By changing the fusion mixture rate on a workstation, the spatial relationship between perilymphatic and endolymphatic space was easily appreciated in both the cochlea and vestibule. In this case, endolymphatic space was enlarged in both the cochlea and vestibule, but the enlargement was especially prominent in the vestibule. Note that CSF in the internal auditory canal is visualized as high signal intensity on the endolymphatic fluid image (G). The signal intensity of perilymphatic space is just suppressed. Thus, the term *endolymphatic image* is only useful for labyrinthine space.

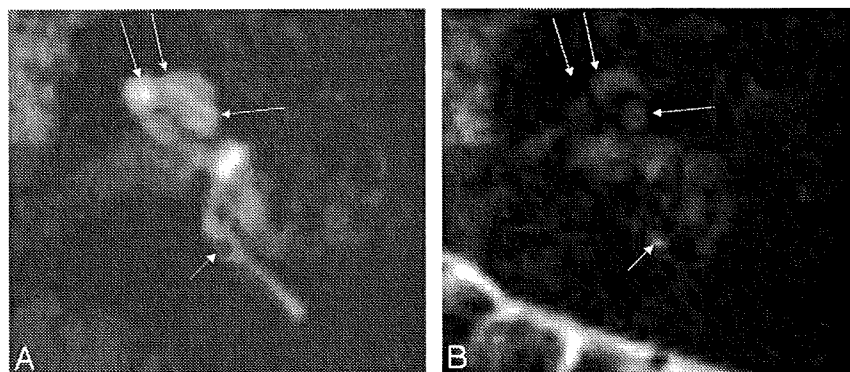


Fig 2. A 43-year-old woman with sudden sensorineural hearing loss in the left ear. All images were obtained 24 hours after the intratympanic injection of Gd-DTPA. A, Perilymphatic fluid image obtained with 3D-FLAIR (9000/128/2500). Areas of low signal intensity in the position of the cochlear duct (arrows) cannot be recognized as the endolymphatic space in the cochlea, probably because of their small size. Note that the endolymphatic space of the posterior ampulla (short arrow) showed low signal intensity. B, Endolymphatic fluid image obtained with a 3D inversion-recovery sequence (9000/128/1000). The endolymphatic space in the cochlea (arrows) cannot be recognized as high signal intensity on this image. Note that the endolymphatic space of the posterior ampulla (short arrow) showed high signal intensity alternatively compared with Fig 2A.

showed the lowest signal intensity in the perilymphatic space. Thus, in all 4 subjects, an inversion time of 1000 ms was selected for 3D-IR imaging of endolymphatic space. Other 3D-IR parameters for endolymphatic imaging were identical to those of 3D-FLAIR. If the size of the endolymphatic space was enlarged, endolymphatic and perilymphatic images were reviewed while referring to 3D-CISS images. The cochlear endolymphatic space is thought to be enlarged if the cochlear duct (endolymphatic space in the cochlea) is bulging toward the perilymphatic space in the scala vestibuli. Also, the vestibular endolymphatic space is thought to be enlarged if the endolymphatic space is larger than the perilymphatic space.

Image Fusion

Endolymphatic (3D-IR with an inversion time of 1000 ms) and perilymphatic images (3D-FLAIR) were fused on a Leonardo workstation (Siemens, Erlangen, Germany). To confirm that the spatial relationship between the perilymphatic and endolymphatic images was anatomically correct, we viewed the fused images on the workstation monitor while changing the weighting scale continuously from pure 3D-IR to pure 3D-FLAIR.

Results

In all patients, an area of low signal intensity in the labyrinth on 3D-FLAIR showed high signal intensity on endolymphatic

images (Fig 1A,B). By scaling the weighting on a fused image, the spatial relationship between the endolymphatic and perilymphatic images was clearly discernible (Fig 1C–G). In the 3 patients with Ménière disease, the endolymphatic space seemed to be enlarged. In the patient with sudden hearing loss, no enlargement of the endolymphatic space was noted (Fig 2).

Discussion

Many researchers⁴ have attempted separate visualization of perilymphatic and endolymphatic fluid space with MR imaging. Direct visualization of the Reissner membrane with use of high spatial-resolution imaging was successful in animals⁵ and human cadavers^{6,7}; however, clear visualization in a living human subject has not been successful. Four hours after intravenous administration of Gd-DTPA in healthy human volunteers, a slight increase in signal intensity was noted in the labyrinth.⁸ However, probably because of a gadolinium concentration that was too low in the perilymphatic space, differentiation between the endolymphatic and perilymphatic space was not achieved. Intratympanic injection of Gd-DTPA and the application of 3D-FLAIR at 3T made the visualization of endolymphatic hydrops possible in vivo.² Although intratympanically administered Gd-DTPA distributes mainly into the perilymphatic fluid space and not into the endolymphatic

space, on 3D-FLAIR the hypointense endolymphatic space was difficult to differentiate from the surrounding bone and air. To delineate the endolymphatic space more clearly and to allow the quantification of the endolymphatic-space volume in the future, the endolymphatic space needs to be visually differentiated not only from the perilymphatic space but also from bone and air. By changing the inversion time, it was possible to separately visualize the endolymphatic and perilymphatic spaces as positive signal intensity. This will allow volume quantification of each space in the future if the spatial resolution is improved. Quantification of each space is important for the objective diagnosis of endolymphatic hydrops and for the monitoring of treatment effectiveness.

Fusion techniques convinced us that each space was separately visualized not only in the cochlea, but also in the vestibule and semicircular canals.

In our study, the labyrinth without intratympanic gadolinium injection (the other side ear) showed uniformly high signal intensity of the whole labyrinth on endolymphatic imaging with use of 3D-IR. This means that the suppression of perilymph on endolymphatic imaging by the present method in the injected side is based on the distribution of gadolinium.

One of the limitations of our presented method was the long acquisition time, 30 minutes for 2 kinds of lymphatic space images. One possibility to obtain endolymphatic images in a shorter period of time is the subtraction of perilymphatic-space images from T2-weighted images. This might allow us to obtain endolymphatic-space images if the subject is nearly motionless during the scans.

The other limitation of our method was the potential rupture of Reissner membrane in a very advanced case of Ménière disease. In such case, contamination of the endolymph and perilymph would occur and endolymphatic space might show low signal intensity on endolymphatic imaging.

Conclusion

By optimizing the inversion time, it was possible to obtain images of the endolymphatic and perilymphatic spaces. The endolymphatic space was differentiated not only from the perilymphatic space, but also from bone and air. This method might open the door to objective evaluation of endolymphatic-space disease.

References

1. Zou J, Pyykkö I, Bjelke B, et al. **Communication between the perilymphatic scalae and spiral ligament visualized by in vivo MRI.** *Audiol Neurootol* 2005;10:145–52
2. Nakashima T, Naganawa S, Sugiura M, et al. **Visualization of endolymphatic hydrops in patients with Meniere's disease.** *Laryngoscope* 2007;117:415–20
3. Griswold MA, Jakob PM, Heidemann RM, et al. **Generalized autocalibrating partially parallel acquisitions (GRAPPA).** *Magn Reson Med* 2002;47:1202–10
4. Niyazov DM, Andrews JC, Strelloff D, et al. **Diagnosis of endolymphatic hydrops in vivo with magnetic resonance imaging.** *Otol Neurotol* 2001;22:813–17
5. Koizuka I, Seo Y, Murakami M, et al. **Micro-magnetic resonance imaging of the inner ear in the guinea pig.** *NMR Biomed* 1997;10:31–34
6. Koizuka I, Seo R, Kubo T, et al. **High-resolution MRI of the human cochlea.** *Acta Otolaryngol Suppl* 1995;520:256–57
7. Koizuka I, Seo R, Sano M, et al. **High-resolution magnetic resonance imaging of the human temporal bone.** *ORL J Otorhinolaryngol Relat Spec* 1991;53:357–61
8. Naganawa S, Komada T, Fukatsu H, et al. **Observation of contrast enhancement in the cochlear fluid space of healthy subjects using a 3D-FLAIR sequence at 3 Tesla.** *Eur Radiol* 2006;16:733–37

Visualization of Endolymphatic Hydrops in Patients With Meniere's Disease

Tsutomu Nakashima, MD; Shinji Naganawa, MD; Makoto Sugiura, MD; Masaaki Teranishi, MD; Michihiko Sone, MD; Hideo Hayashi, MD; Seiichi Nakata, MD; Naomi Katayama, PhD; Ieda Maria Ishida

Objective: Recently, there have been many reports of intratympanic gentamicin therapy for the treatment of intractable Meniere's disease. Intratympanic administration of steroids has also been used to treat sudden sensorineural hearing loss. We attempted to visualize how the intratympanically administered drug enters the inner ear. **Methods:** Gadolinium hydrate diluted eightfold with saline was injected intratympanically through the tympanic membrane using a 23 G needle in nine patients with inner ear diseases. With a 3 Tesla magnetic resonance imaging (MRI) unit, three-dimensional fluid-attenuated inversion recovery (3D-FLAIR) imaging was performed. **Results:** 3D-FLAIR MRI clearly revealed that the gadolinium entered the perilymphatic space and delineated the perilymphatic and endolymphatic spaces of the inner ear. In patients with endolymphatic hydrops, the perilymphatic space surrounding the endolymph was small or had disappeared. Gadolinium appeared first in the scala tympani of the basal turn of the cochlea and the perilymphatic space of the vestibule. One day after the intratympanic injection of gadolinium, the gadolinium was observed in almost all parts of the perilymph. Six days after the intratympanic injection, the gadolinium had almost disappeared from the inner ear. **Conclusion:** We reported the first visualization of endolymphatic hydrops in patients with Meniere's disease. The relationship between the image of the endolymphatic space and functional tests, such as electrocochleography and vestibular-evoked myogenic potential, must be examined in the near future. It is important for the development of intratympanic drug therapies for inner-ear diseases to investigate how the drugs enter and leave the inner ear. **Key Words:** Endolymphatic hydrops,

Meniere's disease, sudden deafness, electrocochleography, vestibular evoked myogenic potential, gadolinium, FLAIR MRI.

Laryngoscope, 117:●●●-●●●, 2007

INTRODUCTION

Although image diagnosis of endolymphatic hydrops may be a key to understanding inner-ear diseases such as Meniere's disease or fluctuating sensorineural hearing loss (HL), imaging the endolymphatic hydrops has not been achieved, except for temporal bone histopathologic specimens in autopsy cases. The composition of the endolymph, with its high potassium and low sodium concentrations, resembles that of the cytosol, in contrast with the composition of the perilymph, which is closer to that of the extracellular medium, with low potassium and high sodium concentrations. However, imaging the endolymphatic space has not been achieved clinically despite these differences in chemical composition. Reissner's membrane, which borders the endolymph and perilymph, is too thin to be visualized.

Electrocochleography (EcochG) and vestibular-evoked myogenic potential (VEMP) have been used to estimate endolymphatic hydrops functionally. The former evaluates the cochlea,¹ and the latter evaluates the vestibule.² Endolymphatic hydrops may occur locally or throughout the entire inner ear. It may also fluctuate with the severity of HL or vertigo attacks. One theory for the cause of vertigo attacks in Meniere's disease is the rupture of the extended Reissner's membrane,³ but the relationship between vertigo attacks and endolymphatic hydrops is not clear. If imaging endolymphatic hydrops becomes possible, a comparison of the images and functional examinations will clarify the significance of the functional examination.

Recently, there have been many reports of intratympanic gentamicin therapy for the treatment of intractable Meniere's disease.^{4,5} Intratympanic administration of steroids has also been used to treat sudden sensorineural HL.^{6,7} These intratympanic drug therapies are based on the passage of the intratympanically administered drug into the inner ear through the round window membrane. However, in some patients, the passage of the drug through the round window membrane is extremely poor because of connective tissue or granulation tissue over the

From the Department of Otorhinolaryngology (T.N., M. SUGIURA, M.T., M. SONE, H.H., S.N., N.K., I.M.I.) and Department of Radiology (S.N.) Nagoya University Graduate School of Medicine, Nagoya, Japan.

Editor's Note: This Manuscript was accepted for publication October 18, 2006.

This study was supported by research grants from the Ministry of Education, Culture, Sports, Science and Technology and the Acute Profound Deafness Committee of the Ministry of Health, Labor and Welfare, Japan.

Send correspondence to Dr. Tsutomu Nakashima, Department of Otorhinolaryngology, Graduate School of Medicine, 65, Tsurumai-cho, Showa-ku, Nagoya 466-8550, Japan. E-mail: tsutomun@med.nagoya-u.ac.jp

DOI: 10.1097/MLG.0b013e31802c300c

round window.⁸ We examined the passage of gadolinium through the round window after its intratympanic administration using magnetic resonance imaging (MRI). The gadolinium entered the perilymphatic space and delineated the perilymphatic and endolymphatic spaces. In patients with Meniere's disease, the extension of the endolymphatic space, called endolymphatic hydrops, could be observed. To our knowledge, this is the first report of the clinical imaging of endolymphatic hydrops.

METHODS

Patients

Nine patients were enrolled in this study. Age, sex, diagnosis, affected side, average hearing level at 500 Hz, 1 kHz, and 2 kHz, presence or absence of vertigo, and the interval between the intratympanic gadolinium injection and MRI are presented in Table I. Four patients had Meniere's disease, four patients had sudden deafness, and one patient had acute low-tone sensorineural HL. The diagnosis of each disease was made according to the criteria described in the literature.⁹⁻¹¹ However, patient no. 4 had nonrotatory episodic vertigo with fluctuating HL. Six patients first underwent MRI 1 or 2 hours after the intratympanic injection of gadolinium. In three patients, the first MRI was taken 1 day after the intratympanic injection, as shown in Table I. Additional MRIs were taken 6 days after the intratympanic injection in three patients (patients no. 4, 6, and 7 in Table I).

In the patients with Meniere's disease, conservative therapy had failed to control their vertigo attacks, and intratympanic gentamicin therapy was tried. In the patients with acute low-tone sensorineural HL and sudden sensorineural HL, hearing recovery was poor after ordinary treatments, so intratympanic injection of steroids was tried. After our evaluation of the intratympanic injection of gadolinium, we planned intratympanic drug therapies.

The protocol of the study was approved by the Ethics Review Committee of Nagoya University School of Medicine (approval numbers 369, 369-2). All patients gave their informed consent to participation in this study. Their written informed consent was attached to the electronic medical record after permission was given by the patient, in accordance with the suggestion of the Ethics Review Committee.

Intratympanic Gadolinium Injection

Gadodiamide hydrate (Omniscan, Daiich Pharmaceutical Co. Ltd, Tokyo, Japan) was diluted eightfold with saline (v/v 1:7). The diluted gadodiamide hydrate was injected intratympanically through the tympanic membrane using a 23 G needle and a 1 mL syringe after the patient was placed in the supine position with his/her head turned approximately 30° away from the sagittal line toward the healthy ear. The gadolinium was injected until a backflow of fluid into the external ear was observed under a microscope. The amount of diluted gadolinium injected was 0.4 to 0.5 mL. After the injection, the patient remained in the supine position for 60 minutes with his/her head turned approximately 60° away from the sagittal line toward the healthy ear.

MRI

MRI scans were performed with a 3 Tesla MR unit (Trio, Siemens, Erlangen, Germany) using a receive-only eight-channel phased-array coil, as described previously.^{12,13} T1-weighted three-dimensional (3D) fast low-angle shot imaging, heavily T2-weighted 3D constructive interference in the steady state imaging, and 3D fluid-attenuated inversion recovery (FLAIR) imaging were performed. For this study, we performed the second 3D-FLAIR with higher in-plane spatial resolution in addition to methods described previously.^{12,13} The scan parameters for the second 3D-FLAIR sequence were as follows: repetition time of 9,000 ms, effective echo time of 128 ms, inversion time of 2,500 ms, constant flip angle echo train with flip angle of 180 degrees for conventional turbo spin echo refocusing echo train, echo train length of 23, matrix size of 384 × 384, 12 axial 2 mm thick slices to cover the labyrinth with a 16 cm square field of view, acceleration factor of two using the parallel imaging technique, generalized autocalibrating partially parallel acquisitions. Voxel size was 0.4 mm × 0.4 mm × 2 mm. The number of excitations was one, and the scan time was 15 minutes.

All MRIs were attached to the electronic medical record and reviewed independently on a liquid crystal display in the Department of Radiology and the Department of Otorhinolaryngology. If there were any discrepancies between the interpretations of the two departments, a consensus was reached by discussion.

TABLE I.
Gadolinium Distribution in Inner Ear After Intratympanic Injection.

Patient No.	Age, Sex	Diagnosis	Side	HL	Vertigo	MRI	Gadolinium Distribution		
							Cochlea	Vestibule	Semicircular Canals
1	57, M	SD	Left	27	No	2 hr	Basal	Whole	Partial
						7 hr	Basal, part of 2nd	Whole	Whole
2	23, M	ALSNHL	Left	12	No	2 hr	Basal	Whole	Partial
3	74, F	SD	Left	85	No	2 hr	Basal	Whole	Partial
4	53, M	Meniere's	Left	35	Yes	2 hr	Basal	Whole	Partial
5	46, M	Meniere's	Left	60	Yes	2 hr	Basal	Faint	No
						1 day	Basal, 2nd	Faint	Faint
6	24, F	SD	Right	68	Yes	1 day	Basal, 2nd	Whole	Whole
7	55, F	Meniere's	Left	58	Yes	1 day	Basal, 2nd, apical	Whole	Whole
8	47, M	SD	Right	97	Yes	1 hr	Basal	Whole	Partial
						1 day	Basal, 2nd, apical	Whole	Whole
9	65, F	Meniere's	Left	63	Yes	1 day	Basal, 2nd	Faint	Faint

SD = sudden deafness; ALSNHL = acute low-tone sensorineural hearing loss; HL = average of hearing level of 500 Hz, 1 kHz, and 2 kHz (dB); MRI = period between intratympanic gadolinium injection and magnetic resonance imaging; gadolinium distribution, "whole" = gadolinium was observed wholly in vestibule or semicircular canals.

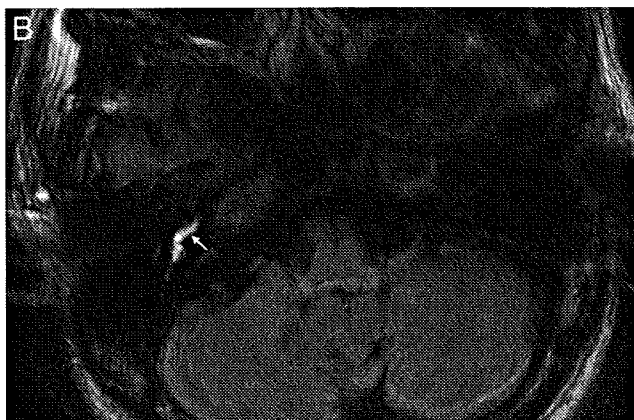
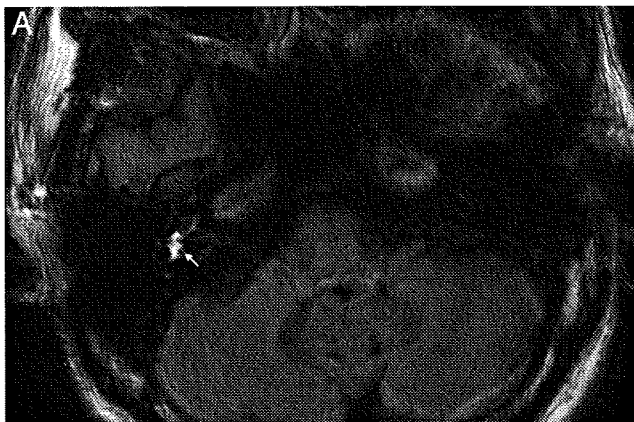


Fig. 1. Three-dimensional fluid-attenuated inversion recovery magnetic resonance images taken 1 hour after intratympanic injection of gadolinium (patient no. 8 in Table I). (A) Gadolinium in vestibule and part of horizontal semicircular canal. Black circle revealed by an arrow in vestibule is crus membranaceum commune. (B) Gadolinium in scala tympani of basal turn of cochlea and vestibule. Arrow indicates scala tympani of basal turn in cochlea.

EcochG

A silver ball electrode was placed on the posteroinferior quadrant of the external ear canal, close to the tympanic membrane. Before the electrode was placed, the skin of the electrode area was cleaned with skin preparation gel for bioelectrical measurements (Skin Pure, Nihonkoden, Tokyo, Japan), and then electrode paste (Biotach, GE Yokogawa Medical, Tokyo, Japan) was spread over the skin area. EcochG was performed while the patient was lying down in a sound-attenuated room. The reference electrode was close to the earlobe, and the ground electrode was on the forehead. The click stimuli were presented four times a second with rarefaction and condensation polarity (Synax 2100, NEC Medical Systems, Tokyo, Japan). The signal was added 500 times through the bandpass filter (100–3,000 Hz). The summing potential (SP) to action potential (AP) ratio was calculated when SP and AP were clear.

VEMP

Surface myogenic potentials in the sternocleidomastoid muscle were added 150 times with a reference electrode over the sternum while clicks (105 dB) were presented to the ipsilateral ear and white noise (75 dB) was presented to the contralateral ear (Synax 2100, NEC Medical Systems, Tokyo, Japan). The ground electrode was on the forehead. The stimulation rate of the clicks was 5 Hz, and the electromyogenic signal was amplified through

a bandpass filter (20–2,000 Hz). The patient was instructed to turn his/her head toward the contralateral side in the sitting position to activate the sternomastoid muscle.

RESULTS

On MRIs taken 1 or 2 hours after the intratympanic injection of gadolinium, the gadolinium was observed in the vestibule, parts of the lateral semicircular canals close to the vestibule, and the scala tympani of the basal turn of the cochlea (Fig. 1). The gadolinium that entered the scala tympani of the cochlea through the round window membrane moved quickly into the vestibule. When the gadolinium entered the perilymph of the vestibule, the endolymphatic space without gadolinium could be seen, as shown in Figure 1A. The utricle and crus membranaceum commune, which is located at the meeting point of anterior and posterior semicircular canal crura, could be seen relatively clearly. However, the saccule, which is smaller than the utricle, was not as clearly visible as the utricle. One day after the intratympanic injection of gadolinium, the gadolinium had infiltrated a wider area in the semicircular canals and the cochlea. These results are summarized in Table I. Figure 2 shows the gadolinium inside the

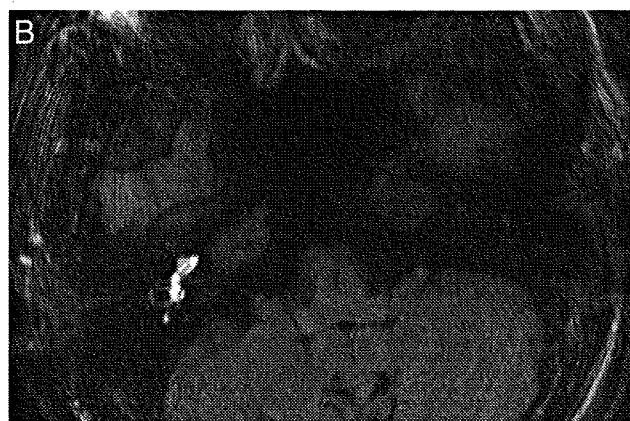


Fig. 2. Three-dimensional fluid-attenuated inversion recovery magnetic resonance images taken 1 day after intratympanic injection of gadolinium (patient no. 8 in Table I). (A) Gadolinium in second and apical turns of cochlea, vestibule, and semicircular canals. Long arrow indicates horizontal semicircular canal and short arrow posterior semicircular canal. (B) Gadolinium in basal and second turns of the cochlea, vestibule, and semicircular canals.

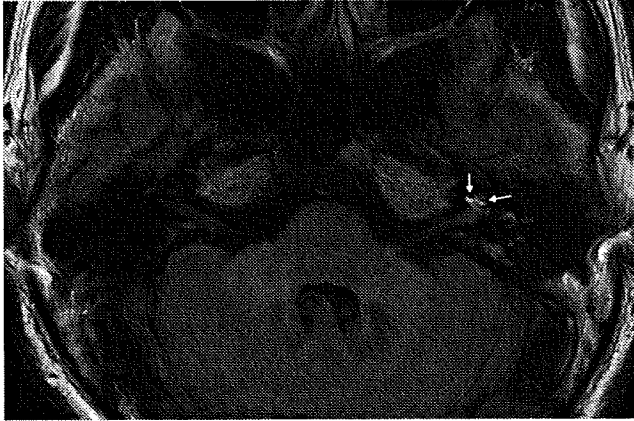


Fig. 3. Three-dimensional fluid-attenuated inversion recovery magnetic resonance image taken 1 day after intratympanic injection of gadolinium (patient no. 5 in Table I). Black areas indicated by arrows are surrounded by gadolinium-filled perilymph. Endolymphatic hydrops in basal turn of cochlea is clearly shown. Gadolinium in vestibule and semicircular canals is faintly visible.

inner ear 1 day after the intratympanic injection of gadolinium. In Figure 2, the border between the perilymph and endolymph inside the vestibule is visible, as it was on the MRI taken 1 hour after the intratympanic injection of gadolinium. This means that the entrance of the gadolinium into the endolymph from the perilymph was negligible in the vestibule on the first day. However, the gadolinium moved toward upper turns of the cochlea during this period, and the scala vestibuli and scala media became visible (Fig. 2).

In patients no. 5 and 9, who had Meniere's disease, gadolinium was barely visible in the vestibule because endolymphatic hydrops occupied the perilymphatic space. In patient no. 5, the gadolinium was only faintly visible in the vestibule 1 day after the intratympanic injection of gadolinium, similarly 2 hours after the intratympanic injection. In the cochlea, the gadolinium moved toward the upper turn, and the endolymphatic hydrops inside the perilymphatic space filled with the gadolinium was observed in the basal turn of the cochlea (Fig. 3). It is clear that the endolymphatic space in Figure 3 is significantly enlarged compared with that in Figure 2. In Figure 3, the gadolinium does not reach the helicotrema. Accordingly, the gadolinium appeared in the scala vestibule of the basal turn by way of the lateral wall of the cochlea not by way of the helicotrema. In patient no. 5, VEMP was absent, and the SP/AP ratio on EcochG was high (48%). This patient had frequent drop attacks despite the disappearance of rotatory vertigo after earlier intratympanic gentamicin therapy. In patient no. 9, endolymphatic hydrops was also observed in the cochlea in the MRI taken 1 day after the intratympanic gadolinium injection. In patient no. 9, VEMP was absent, and AP in EcochG could not be obtained clearly. This patient had rotatory vertigo attacks even after intratympanic gentamicin therapy.

One day after the intratympanic injection of gadolinium, the gadolinium-filled perilymphatic space was small in the vestibule of patient no. 7, who had Me-

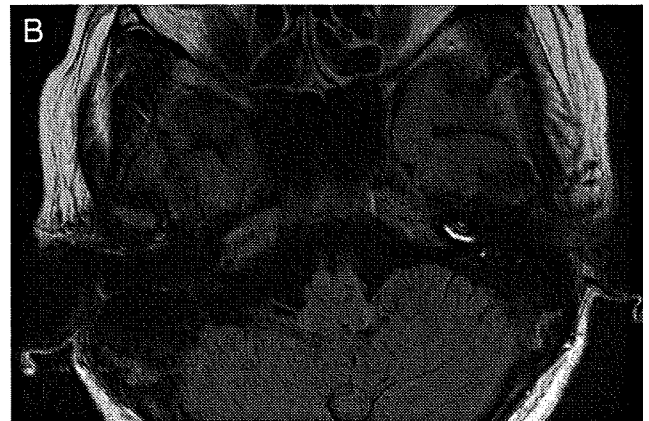
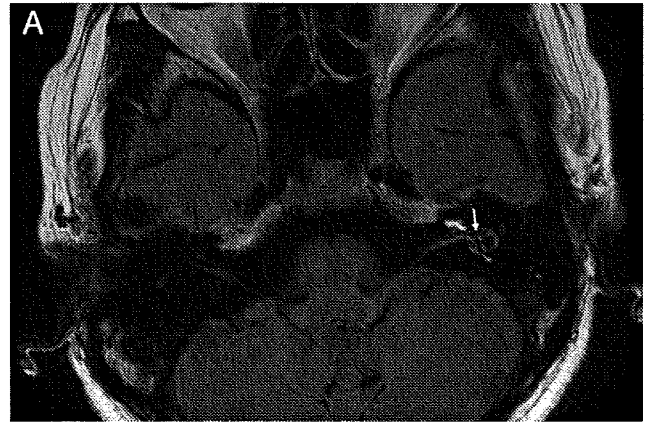


Fig. 4. Three-dimensional fluid-attenuated inversion recovery magnetic resonance images taken 1 day after intratympanic injection of gadolinium (patient no. 7 in Table I). (A) Gadolinium in basal and second turns of cochlea, vestibule, and semicircular canals. Large black areas in vestibule represent vestibular endolymphatic hydrops (indicated by arrow). (B) Gadolinium in three turns of cochlea. Almost all gadolinium was present in scala tympani of cochlea.

niere's disease, because of vestibular endolymphatic hydrops (Fig. 4A). It is clear that the endolymphatic space in the vestibule in Figure 4A is larger than that in Figure 2A. In this patient, each cochlear turn was visualized separately because almost all gadolinium was observed only in the scala tympani in the cochlea (Fig. 4B). It appears that gadolinium that passes through the helicotrema or the lateral wall toward the scala vestibuli was blocked by the extended endolymphatic hydrops in the cochlea. This patient had an extremely high SP/AP ratio (100%) without VEMP.

VEMP was present in six patients, except patients no. 5, 7, and 9. The amplitude ratio of the VEMP on the affected side to that on the healthy side was more than 75% in these six patients. No high SP/AP ratios on EcochG were observed except for patients no. 5 and 7, although EcochG was not performed in patients no. 2 or 3. The SP/AP ratio could not be obtained because of low AP amplitude in patients no. 6, 8, and 9.

Six days after the intratympanic injection of gadolinium, MRI was performed in three patients (no. 4, 6, and 7 in Table I). At this time, the gadolinium had almost dis-

appeared from the inner ear. However, there was interpatient variability in the pattern of gadolinium disappearance. In one patient with Meniere's disease (patient no. 4), the residual gadolinium was visible compared with that in the other two patients.

No adverse effects of the intratympanic injection of gadolinium were observed. There was also no change in tinnitus.

DISCUSSION

Gadolinium was not visible in the tympanic cavity 1 hour after the transtympanic injection. Gadolinium in the tympanic cavity might have quickly disappeared through the auditory tube. The movement of the gadolinium in the middle ear needs to be studied further after investigation of suitable gadolinium concentration for 3D-FLAIR MRI.

Because intratympanically administered contrast enhancement material moves first into the perilymphatic space of the inner ear, precise MRIs taken soon after intratympanic administration can reveal the border of the endolymph and perilymph. Therefore, we could visualize endolymphatic hydrops in humans. In an MRI taken 1 day after the intratympanic injection of gadolinium, the border of the perilymph and endolymph was clearly visible, and the gadolinium was observed almost wholly inside the inner ear. Therefore, we consider that MRI undertaken 1 day after the intratympanic injection of gadolinium provides maximum information to observe endolymphatic hydrops both in the cochlea and vestibule.

Using 1.5 Tesla T1 MRI, Zou et al.¹⁴ have previously shown that intratympanically administered gadolinium moved into the inner ears of two patients. Our study with 3 Tesla 3D-FLAIR MRI provided very clear images and made possible the visualization of endolymphatic hydrops, although the concentration of the gadolinium injected into the tympanic cavity was one eighth that of the original gadolinium solution. Our T1 MRIs taken at 3 Tesla revealed the distribution of gadolinium in the inner ear. However, the border of the endolymph and perilymph was markedly clearer on 3D-FLAIR MRI than on T1 MRI. FLAIR sequences sometimes demonstrate hemorrhage or a high concentration of protein, which are difficult to detect with T1- or T2-weighted MRI.^{12,13} Two-dimensional (2D)-FLAIR sequences show flow-related artifacts caused by the inflow of cerebrospinal fluid (CSF) from outside the slice volume, which sometimes obscures the pathology. We have reported previously that CSF-related flow artifacts are significantly reduced on 3D-FLAIR images relative to those on 2D-FLAIR images.¹⁵ The 3D-FLAIR sequence allows the detection on serial, thin slices of conditions that mimic other pathologies of the inner ear, such as inner-ear hemorrhage or high concentrations of protein.¹³

In three patients with Meniere's disease without VEMP, the movement of gadolinium into the vestibule was restricted. It is assumed that the extremely large endolymphatic hydrops in the vestibule prevented the movement of the gadolinium from the scala tympani of the

cochlea to the vestibule. A decrease in or disappearance of VEMP, which is a function of the saccule, is associated with endolymphatic hydrops in the vestibule.² The relationship between the image of the endolymphatic space and functional tests, such as EcochG and VEMP, must be examined further in the near future.

After 6 days from the intratympanic injection of gadolinium, the gadolinium had almost disappeared from the inner ear. However, there was interpatient variability in the pattern of gadolinium disappearance. The pattern or speed of the disappearance may be associated with circulation of the inner ear. It is important for the development of intratympanic drug therapies for inner-ear diseases to investigate how the drugs enter and leave the inner ear.

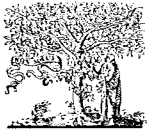
CONCLUSIONS

1. Intratympanically administered gadolinium moves quickly into the scala tympani of the basal turn of the cochlea and the perilymphatic space of the vestibule. One day after the intratympanic administration, the gadolinium appears in almost all parts of the perilymph inside the inner ear.
2. With use of 3 Tesla 3D-FLAIR MRI, the size of endolymphatic space can be evaluated clearly after the intratympanic gadolinium administration.
3. Extremely large endolymphatic hydrops in the vestibule may prevent the intratympanically administered drug from moving into the vestibule and semicircular canals. This should be taken into consideration for intratympanic gentamicin therapy in patients with Meniere's disease.

BIBLIOGRAPHY

1. Ferraro JA, Durrant JD. Electrocochleography in the evaluation of patients with Meniere's disease/endolymphatic hydrops. *J Am Acad Audiol* 2006;17:45-68.
2. Lin MY, Timmer FC, Oriol BS, et al. Vestibular evoked myogenic potentials (VEMP) can detect asymptomatic saccular hydrops. *Laryngoscope* 2006;116:987-992.
3. Valk WL, Wit HP, Albers FW. Rupture of Reissner's membrane during acute endolymphatic hydrops in the guinea pig: a model for Meniere's disease? *Acta Otolaryngol* 2006;126:1030-1035.
4. Cohen-Kerem R, Kisilevsky V, Einarson TR, et al. Intratympanic gentamicin for Meniere's disease: a meta-analysis. *Laryngoscope* 2004;114:2085-2091.
5. Smith WK, Sankar V, Pfeleiderer AG. A national survey amongst UK otolaryngologists regarding the treatment of Meniere's disease. *J Laryngol Otol* 2005;119:102-105.
6. Slattery WH, Fisher LM, Iqbal Z, et al. Intratympanic steroid injection for treatment of idiopathic sudden hearing loss. *Otolaryngol Head Neck Surg* 2005;133:251-259.
7. Alles MJ, der Gaag MA, Stokroos RJ. Intratympanic steroid therapy for inner ear diseases, a review of the literature. *Eur Arch Otorhinolaryngol* 2006;263:791-797.
8. Johansson U, Hellstrom S, Anniko M. Round window membrane in serous and purulent otitis media. Structural study in the rat. *Ann Otol Rhinol Laryngol* 1993;102:227-235.
9. Committee on Hearing and Equilibrium. Committee on hearing and equilibrium guidelines for the diagnosis and evaluation of therapy in Meniere's disease. *Otolaryngol Head Neck Surg* 1995;113:181-185.

10. Nomura Y. Diagnostic criteria for sudden deafness, mumps deafness and perilymphatic fistula. *Acta Otolaryngol Suppl* 1988;456:7-8.
11. Abe T, Tsuiki T, Murai K, Goto M, et al. Review of the evaluation criteria for low tone sudden deafness. *Nippon Jibiinkoka Gakkai Kaiho* 1992;95:7-14.
12. Naganawa S, Komada T, Fukatsu H, et al. Observation of contrast enhancement in the cochlear fluid space of healthy subjects using a 3D-FLAIR sequence at 3 Tesla. *Eur Radiol* 2006;16:733-737.
13. Sugiura M, Naganawa S, Teranishi M, Nakashima T. Three-dimensional fluid-attenuated inversion recovery magnetic resonance imaging findings in patients with sudden sensorineural hearing loss. *Laryngoscope* 2006;116:1451-1454.
14. Zou J, Pyykkö I, Bjelke B, et al. Communication between the perilymphatic scalae and spiral ligament visualized by in vivo MRI. *Audiol Neurootol* 2005;10:145-152.
15. Naganawa S, Koshikawa T, Nakamura T, et al. Comparison of flow artifacts between 2D-FLAIR and 3D-FLAIR sequences at 3 T. *Eur Radiol* 2004;14:1901-1908.



ELSEVIER

Auris Nasus Larynx 35 (2008) 269–272

AURIS NASUS
LARYNX
INTERNATIONAL JOURNAL
OF ORL & HNS

www.elsevier.com/locate/anl

Three-dimensional fluid-attenuated inversion recovery magnetic resonance imaging findings in a patient with cochlear otosclerosis

Makoto Sugiura^{a,*}, Shinji Naganawa^b, Michihiko Sone^a,
Tadao Yoshida^a, Tsutomu Nakashima^a

^a Department of Otorhinolaryngology, Nagoya University Graduate School of Medicine 65,
Tsurumai-cho, Showa-ku, Nagoya 466-8550, Japan

^b Department of Radiology, Nagoya University Graduate School of Medicine, Nagoya, Japan

Received 18 December 2006; accepted 18 April 2007

Available online 5 September 2007

Abstract

A 51-year-old man had progressive hearing loss over more than 15 years. He had bilateral sensorineural hearing loss (SNHL). Computed tomography (CT) showed extensive bilateral demineralization of the cochlear capsule, which is characteristic of diffuse cochlear otosclerosis. Three-dimensional fluid-attenuated inversion recovery (3D-FLAIR) of magnetic resonance imaging before enhancement revealed high signals in the cochlea and vestibule. Postcontrast 3D-FLAIR revealed enhancement of the basal turn of the left cochlea. This is the first published case of the breakdown of the blood–labyrinth barrier in a patient with cochlear otosclerosis. Our findings suggest that the breakdown of the blood–labyrinth barrier is associated with a part of SNHL in cochlear otosclerosis.

© 2007 Elsevier Ireland Ltd. All rights reserved.

Keywords: Cochlear otosclerosis; Sensorineural hearing loss; Fluid-attenuated inversion recovery (FLAIR); Magnetic resonance imaging (MRI)

1. Introduction

Radiological studies are important tools in demonstrating the lesions of cochlear otosclerosis. Although high-resolution computed tomography (CT) can show otosclerosis within the otic capsule, some investigators have recently reported the usefulness of magnetic resonance imaging (MRI), especially in the diagnosis of active otosclerosis (otospongiosis) [1–3]. However, the pathophysiological mechanisms of sensorineural hearing loss (SNHL) in cochlear otosclerosis are unclear. Here, we describe a patient with cochlear otosclerosis in whom three-dimensional fluid-attenuated inversion recovery (3D-FLAIR) MRI showed the breakdown of the blood–labyrinth barrier.

2. Case report

A 35-year-old man experienced left progressive SNHL without vertigo. At the age of 43 years, he presented with right acute SNHL with vertigo. There was no remarkable personal or family history. Clinical examination revealed no significant findings. Schwartz's sign was not noted at that time. Pure tone audiometry showed 60 dB (the average of 500, 1000, and 2000 Hz) in the right ear and 80 dB in the left ear, with no apparent air–bone gap. The speech discrimination score was 90% at 80 dB in the right ear and 55% at 100 dB in the left ear. Distortion product otoacoustic emissions (DPOAEs) were absent in both ears. MRI without FLAIR and without enhancement showed normal findings at that time. He was treated with hydrocortisone at 200 mg/d (first to fourth days of admission) and 100 mg/d (fifth to eighth days), and his hearing improved to an average of 43 dB in the right ear.

When he was 48 years old, he experienced hearing deterioration in the right ear, without vertigo. The audiogram

* Corresponding author. Tel.: +81 52 744 2323; fax: +81 52 744 2325.
E-mail address: makotos@med.nagoya-u.ac.jp (M. Sugiura).

showed 63 dB in the right ear and 92 dB in the left ear. He underwent CT and MRI to evaluate his ears. CT showed extensive bilateral demineralization of the cochlear capsule, which is characteristic of diffuse cochlear otosclerosis (Fig. 1). Enhanced T1-weighted MRI showed bilateral enhancement of the soft tissue in the cochlear capsule, instead of the normal signal void from the bone. He was diagnosed with cochlear otosclerosis. Bilateral Schwartze's sign was noted at this time. He was treated with hydrocortisone at 200 mg/d (first to fourth days of admission) and 100 mg/d (fifth to eighth days), but there was no improvement in hearing on the right.

In May 2006, at the age of 51, the patient experienced sudden deterioration of hearing in the right ear, without vertigo. The audiogram showed 80 dB in the right ear and 112 dB in the left ear. MRI three-dimensional fluid-attenuated inversion recovery (3D-FLAIR) images, before enhancement, revealed bilateral faint high-signal areas in the cochleas and vestibules (Fig. 2a). MRI scans were performed with a 3-T MR (Trio, Siemens, Erlangen, Germany) using a receive-only eight-channel phased-array coil. 3D-FLAIR was obtained before and after the administration of a single dose of gadolinium. Contrast-enhanced 3D-FLAIR was initiated 7 min after the gadolinium was administered, so that

the contrast of 3D-FLAIR was determined approximately 10 min after the administration of gadolinium. The MRI protocols and the film settings have been described in detail in a previous report [4]. Postcontrast 3D-FLAIR revealed bilateral enhancement of the cochleas, especially in the basal turn of the left cochlea (Fig. 2b). Enhanced T1-weighted MRI revealed bilateral enhancement of the soft tissue around the cochlea, similar to the MRI findings 3 years ago. However, high-signal areas on 3D-FLAIR after enhancement were not detected by T2- and T1-weighted MRI (Fig. 2c). He was treated with 30 mg/d of prednisolone, but there was no significant improvement in hearing. The steroid dosage was reduced to 20 mg/d of prednisolone, and he experienced continued hearing deterioration in the right ear.

3. Discussion

In this case, postcontrast 3D-FLAIR revealed enhancement of the inner ear fluid, while conventional postcontrast MRI could only show enhancement of the decalcified area (or otosclerotic lesion) in otosclerosis. This enhancement suggested breakdown of the blood–labyrinth barrier. This is the first report to show breakdown of the blood–labyrinth barrier in a patient with cochlear otosclerosis, the identification of which has been made possible by the new method of 3D-FLAIR. These MRI findings may help to clarify the cause of hearing deterioration in a part of patients with cochlear otosclerosis.

The FLAIR sequence is a part of the routine protocol for MRI of the brain [5]. Subtle high-signal areas in the cerebrospinal fluid (CSF) can be an indicator of subarachnoid hemorrhage, meningitis, or acute infraction. The FLAIR sequence sometimes demonstrates hemorrhage or a high concentration of protein, which are difficult to detect by T1- and T2-weighted MRI. The two-dimensional (2D)-FLAIR sequence shows flow-related artifacts caused by the inflow of CSF from outside the slice volume, which sometimes obscures any pathology present. We have reported previously that CSF-related flow artifacts are significantly lower on 3D-FLAIR images than on 2D-FLAIR images [5]. The 3D-FLAIR sequence allows the detection on serial thin slices of conditions that mimic other pathologies of the inner ear, such as inner-ear hemorrhage and high concentrations of protein. We have recently reported high signals in the affected inner ears of patients with idiopathic sudden SNHL using 3D-FLAIR [4]. In that report, one of eight patients with sudden SNHL showed gadolinium enhancement in the affected cochlea on 3D-FLAIR, which suggested breakdown of the blood–labyrinth barrier. In this study, postcontrast 3D-FLAIR showed bilateral enhancement in the cochleas, especially in the basal turn of the left cochlea. The enhancement seen in both ears suggested breakdown of the blood–labyrinth barrier. Furthermore, the MRI findings suggested that the breakdown in the left ear was more severe than that in the right ear. We have recently



Fig. 1. Computed tomography. This image shows severe demineralization (arrows) around the left cochlea, which is characteristic of diffuse cochlear otosclerosis.

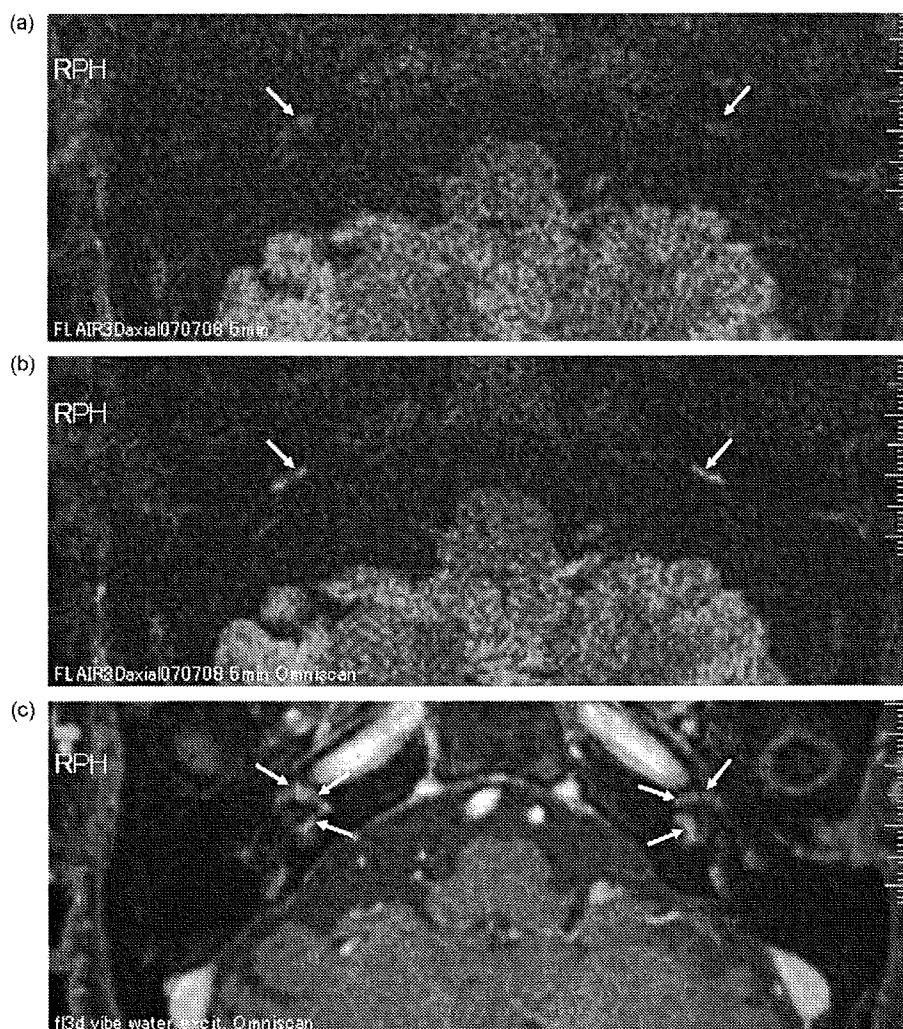


Fig. 2. Axial magnetic resonance imaging (MRI). (a) Three-dimensional fluid-attenuated inversion recovery (3D-FLAIR) images before enhancement. Bright signals are faintly visible bilaterally in the cochleas (arrows). (b) 3D-FLAIR after enhancement. Gadolinium enhancement is seen bilaterally in the cochleas (arrows), especially in the basal turn of the left cochlea. (c) Enhanced T1-weighted MRI. Bilateral enhancement of the soft tissue around the cochleas is seen (arrows). However, the high-signal areas visualized on 3D-FLAIR after enhancement were not detected.

reported that the cochlear fluid in normal subjects is enhanced on 3D-FLAIR imaging 4 h after gadolinium injection, but normal subjects show no enhancement on 3D-FLAIR 10 min after gadolinium injection [6]. From these results, it is clear that the positive findings in this 3D-FLAIR study are significant. We have demonstrated that 3D-FLAIR is a very useful tool in the detection of minute abnormalities in the inner ear that are not detected by conventional T1- or T2-weighted MRI.

The enhancement of the soft tissue around the cochlea which was detected by T1-weighted MRI is presumed to be owing to contrast pooling in the blood vessels of otosclerotic foci [3]. In contrast to this, the cochlea enhancement which was detected by 3D-FLAIR is presumed to be owing to the increased permeability of blood vessels [4].

Schwartz's sign, which indicates proliferation or dilatation of the blood vessels in the promontory, is occasionally observed in cochlear otosclerosis. This sign has been reported

to be associated with increased blood flow to the promontory [7]. In patients with cochlear otosclerosis, temporal bone histopathology shows significant dilatation of blood vessels, including the spiral modiolar vein and the vein of the cochlear aqueduct [8]. The inner ear artery (the labyrinthine artery), usually a branch of the anterior inferior cerebellar artery, nourishes the inner ear. The middle ear is usually supplied by the carotid arterial system. Despite their close anatomical relationship, there is no functional anastomosis of blood vessels between the middle and inner ear [9]. Vascular shunts between the cochlea and the surrounding bone, which have been described histologically in cochlear otosclerosis, are considered unique [8,10]. Histopathological studies of temporal bone in cochlear otosclerosis have suggested that venous congestion occurs inside the cochlea.

It is well known that one of the effects of steroids is to suppress the increased permeability of blood vessels. It is possible that the effect of steroids in this case was associated

with the suppression of permeability of the inner-ear blood vessels. This report is important in suggesting that a part of progressive SNHL in cochlear otosclerosis is associated with increased permeability of blood vessels. Further studies are needed to clarify the relationship between the MRI findings and hearing loss in cochlear otosclerosis. We believe that our study will help further understanding of the pathophysiology of cochlear otosclerosis.

Acknowledgements

This study was supported by research grants from the Ministry of Health, Labour and Welfare and from the Ministry of Education, Culture, Sports, Science and Technology of Japan.

References

- [1] Mark AS, Seltzer S, Harnsberger HR. Sensorineural hearing loss: more than meets the eye? *AJNR Am J Neuroradiol* 1993;14:37–45.
- [2] Saunders JE, Derebery MJ, Lo WW. Magnetic resonance imaging of cochlear otosclerosis. *Ann Otol Rhinol Laryngol* 1995;104:826–9.
- [3] Ziyeh S, Berlis A, Ross UH, Reinhardt MJ, Schumacher M. MRI of active otosclerosis. *Neuroradiology* 1997;39:453–7.
- [4] Sugiura M, Naganawa S, Teranishi M, Nakashima T. Three-dimensional fluid-attenuated inversion recovery magnetic resonance imaging findings in patients with sudden sensorineural hearing loss. *Laryngoscope* 2006;116:1451–4.
- [5] Naganawa S, Koshikawa T, Nakamura T, Kawai H, Fukatsu H, Ishigaki T, et al. Comparison of flow artifacts between 2D-FLAIR and 3D-FLAIR sequences at 3 T. *Eur Radiol* 2004;14:1901–8.
- [6] Naganawa S, Komada T, Fukatsu H, Ishigaki T, Takizawa O. Observation of contrast enhancement in the cochlear fluid space of healthy subjects using a 3D-FLAIR sequence at 3 T. *Eur Radiol* 2006;16:733–7.
- [7] Nakashima T, Sone M, Fujii H, Teranishi M, Yamamoto H, Otake H, et al. Blood flow to the promontory in cochlear otosclerosis. *Clin Otolaryngol* 2006;31:110–5.
- [8] Ruedi L, Spoendlin H. Pathogenesis of sensorineural deafness in otosclerosis. *Ann Otol Rhinol Laryngol* 1966;75:525–52.
- [9] Nakashima T, Naganawa S, Sone M, Tominaga M, Hayashi H, Yamamoto H, et al. Disorders of cochlear blood flow. *Brain Res Rev* 2003;43:17–28.
- [10] Johnsson LG, Pyykkö I, Pollak A, Gleeson M, Felix H. Cochlear vascular pathology and hydrops in otosclerosis. *Acta Otolaryngol* 1995;115:255–9.

Vestibular aqueduct in sudden sensorineural hearing loss

M SUGIURA, S NAGANAWA*, I M ISHIDA, M TERANISHI, S NAKATA, T YOSHIDA, T NAKASHIMA

Abstract

Objective: To evaluate the vestibular aqueduct in patients with sudden sensorineural hearing loss.

Methods: We evaluated 19 patients (12 men and seven women; age range, 22–79 years) with unilateral sudden sensorineural hearing loss, using computed tomography and magnetic resonance imaging. All these patients had unilateral sudden sensorineural hearing loss. We also evaluated 47 control subjects (22 men and 25 women; age range, 22–79 years).

Results: In sensorineural hearing loss affected ears, the width of the vestibular aqueduct at the midpoint and at the operculum was significantly greater than that in contralateral ears or in control ears. The width of the vestibular aqueduct at the midpoint and the operculum did not correlate with the audiometric threshold or the audiogram configuration. Contrast enhancement of the ipsilateral endolymphatic sac was observed in 17 of 19 patients with sudden sensorineural hearing loss (89 per cent). Eleven of these 17 patients also showed enhancement on the contralateral side, but no patient showed enhancement only on the contralateral side. In sensorineural hearing loss affected ears, the width of the vestibular aqueduct did not differ significantly between those patients with and without enhancement.

Conclusions: The vestibular aqueducts of sudden sensorineural hearing loss affected ears are wider than those of controls. Precise imaging and evaluation of the inner ear is essential when investigating the pathological conditions responsible for sudden sensorineural hearing loss.

Key words: Sudden Hearing Loss; Endolymphatic Duct; Endolymphatic Sac; Computed Tomography; Magnetic Resonance Imaging

Introduction

The aetiology of sudden sensorineural hearing loss (SNHL) includes various pathophysiological processes. Many investigators have studied the aetiology of SNHL and identified such causal factors as: perilymphatic fistula, viral infections,¹ autoimmune disorders,¹ asymptomatic mumps infection,² inner-ear haemorrhage,³ inner-ear anomaly⁴ and disordered blood flow.⁵

Temporal bone⁶ and computed tomography (CT) studies⁷ have demonstrated that the width of the vestibular aqueduct is smaller in Ménière's disease patients than in normal controls. However, the width of the vestibular aqueduct in patients with sudden SNHL has not been reported. This study was conducted to evaluate the width of the vestibular aqueduct in patients with sudden SNHL. We have previously reported that, in patients with sudden SNHL, the frequency of contrast enhancement of the endolymphatic sac was significantly greater than that in control subjects.⁸ In the present study, we attempted to investigate the relationship between the width of the vestibular aqueduct and the presence of endolymphatic sac enhancement, in

patients with sudden SNHL, in association with the prognosis for the patient's hearing.

Patients and methods

A total of 19 patients (12 men and seven women; age range, 22–79 years; overall mean age \pm standard deviation (SD) = 53.0 \pm 14.7 years) and 47 control subjects without SNHL were evaluated prospectively. All the patients attended our university hospital between April 2005 and April 2006. All patients had unilateral sudden SNHL. The criteria for sudden SNHL in this study were: patients being able to describe the day of onset of sudden SNHL for which no cause was known; no hearing loss being observed before the onset of sudden SNHL; and hearing loss occurring in less than three days. We excluded patients with fluctuating hearing loss or progressive hearing loss. All patients were examined using both unenhanced and enhanced magnetic resonance imaging (MRI) and CT. All 47 control subjects suffered from unilateral chronic otitis media and were evaluated with CT.

Audiological findings

Throughout the study, the same audiometer (Model AA-79S, Rion, Tokyo, Japan) was used to evaluate hearing levels in a sound-insulated chamber. Serial audiograms were compared with tympanograms and speech discrimination scores, when available. The average hearing level was expressed as the average score at three frequencies (500, 1000 and 2000 Hz). If the patients did not respond to the maximum sound level produced by the audiometer, we defined the threshold as 5 dB added to the maximum level.

The outcome of sudden SNHL was evaluated using the criteria of the Ministry of Health and Welfare of Japan.⁹ By these criteria, the average hearing level is calculated as the average of the hearing levels measured at 250, 500, 1000, 2000 and 4000 Hz. Recovery was ranked as follows:⁸ no change = improvement in hearing of less than 10 dB on average; slight improvement = improvement in hearing of 10 dB or more but less than 30 dB on average; marked improvement = improvement in hearing of 30 dB or more on average; and complete recovery = all five frequencies of the final audiogram were 20 dB or less, or improvement to the same degree of hearing as observed in the contralateral ear. The prognosis score was assigned as follows: zero = no change; one = slight improvement; and two = marked improvement or complete recovery.

Magnetic resonance imaging

From April 2005 to November 2005, MRI scans were performed using a 1.5-Tesla MR system (Visart, Toshiba, Tokyo, Japan) with bilateral, quadrature surface, phased-array coils over both ears. The MRI protocols have been described in detail in previous reports.^{8,10,11} The film settings were the same as those previously reported.⁸ From December 2005, MRI scans were performed with a 3-Tesla MR system (Trio, Siemens, Erlangen, Germany) using a receive-only, eight-channel, phased-array coil. The MRI protocols and the film settings have been described in detail in a previous report.¹²

Endolymphatic sac enhancement

Two observers, who were blinded to patients' medical histories, reviewed all images independently with regard to contrast enhancement in the vicinity of the intraosseous or extraosseous endolymphatic sac. Contrast enhancement was judged to be present when comparison of the pre- and post-contrast-enhanced T1-weighted images showed the appearance of a distinct linear or band-like area of increased signal intensity more than 2 mm in length, after administration of the contrast material. The image interpretation has been described in detail in a previous report.⁸ 'Enhancement' of the sac does not mean a glittering sac, but the appearance of increased signal intensity after administration of the contrast material. Contrast enhancement in the vicinity of the endolymphatic sac

was recorded as present or absent. If there was any disagreement between the observers, a consensus was reached by discussion. The relationship between enhancement and the period from the onset of hearing loss to the MRI examination was also evaluated. The relationship between enhancement and the patient's outcome with regard to hearing was also assessed.

Computed tomography

All CT images were obtained using a CT system with four detector rows (Aquillion, Toshiba) by 0.5 mm collimation, with a 512 × 512 matrix. The film settings have been described in detail in a previous report.¹³

Vestibular aqueduct measurement

The width of the aqueduct was measured at two points: at the operculum (i.e. a line perpendicular to the posterior surface of the petrous pyramid and extending to the most lateral or postlateral pixel in the medial wall of the operculum) and at the midpoint (i.e. the halfway point between the operculum and the posterior wall of the crus commune or vestibule), according to the method of Madden *et al.* (Figure 1).¹⁴

Two observers, who were blinded to the patients' medical histories, reviewed all images independently with regard to the width of the vestibular aqueduct. The width of the vestibular aqueduct was recorded as the average of the observers' measurements. If there was a large difference between these observations, a consensus was reached by discussion.

Statistical analysis

The width of the vestibular aqueduct at the midpoint and operculum was assessed, comparing: patients with sudden SNHL and control subjects; patients' affected and non-affected ears; and ears affected with otitis media and contralateral ears, in control

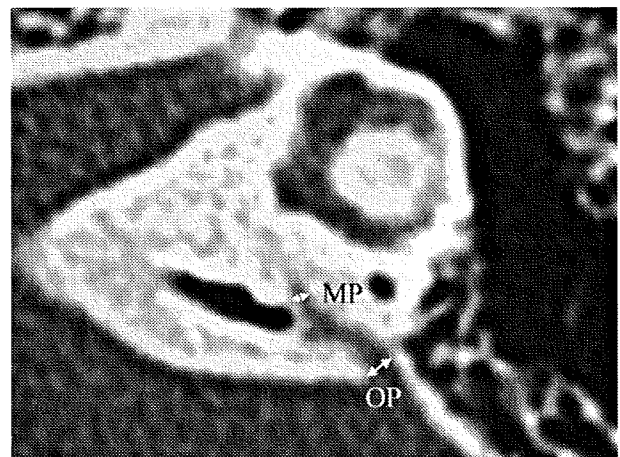


FIG. 1

Axial computed tomographic scan showing measurement of the vestibular aqueduct width. MP = midpoint; OP = operculum

subjects. The relationship between the width of the vestibular aqueduct and the audiometric threshold (in each of the initial and final audiograms) or the audiogram configuration was evaluated. The relationship between contrast enhancement of the endolymphatic sac and the width of the vestibular aqueduct in patients with SNHL was also evaluated.

The average prognosis scores were compared for patients with and without enhancement. The relationship between the width of the vestibular aqueduct and the prognosis with regard to hearing was assessed.

These statistical analyses were performed using chi-square testing, Mann-Whitney *U* testing and Pearson correlation coefficients.

Results

The results for contrast enhancement of the endolymphatic sac and for the width of the vestibular aqueduct are presented in Table I, together with data on hearing outcomes and on the length of time from the onset of hearing loss to the MRI examination.

The width of the vestibular aqueduct at the midpoint and operculum in the SNHL-affected ears was significantly greater than that in the contralateral ears (midpoint, *p* < 0.05; operculum, *p* < 0.05) and that in the ears of control subjects (midpoint, *p* < 0.05; operculum, *p* < 0.0005) (Table II and Figure 2). The width of the vestibular aqueduct at the midpoint and the operculum did not differ significantly, comparing contralateral ears in sudden SNHL and control ears (Table II and Figure 2). In control subjects, the width of the

TABLE II

VESTIBULAR AQUEDUCT WIDTH AT MIDPOINT AND OPERCULUM

Ear	VA width (average ± SD; mm)	
	MP	OP
Affected, in sudden SNHL	0.6 ± 0.2	1.0 ± 0.3
Unaffected, in sudden SNHL	0.5 ± 0.2	0.8 ± 0.3
Affected, in control	0.5 ± 0.1	0.7 ± 0.2
Unaffected, in control	0.6 ± 0.2	0.8 ± 0.2

VA = vestibular aqueduct; SD = standard deviation; MP = midpoint; OP = operculum; SNHL = sensorineural hearing loss

vestibular aqueduct at the midpoint and operculum was not significantly different, comparing the chronic otitis media affected ears and the contralateral ears (Table II).

The average hearing level (in both initial and final audiograms) showed no correlation with the vestibular aqueduct width. Audiometric configurations in this study were flat in 13 ears (68 per cent) and up-sloping in five ears (26 per cent). A down-sloping configuration was found in one ear (5 per cent). We then analysed the audiogram configuration for each patient and found no correlation with the vestibular aqueduct width. Four out of 19 patients had vertigo. No relationship between the presence of vertigo and the width of the vestibular aqueduct was found.

The MRI scans for nine patients (cases one to nine in Table I) were performed using a 1.5-Tesla MR system, and the MRI scans for 10 patients (cases 10-19) were performed using a 3-Tesla MR system. In patients with sudden SNHL, the frequency of

TABLE I

CLINICAL AND IMAGING RESULTS FOR PATIENTS WITH SUDDEN SENSORINEURAL HEARING LOSS

Case	Age (yr), gender	Side	Initial/final hearing level* (dBA)	Audiogram configuration	Vertigo?	MP width (mm)	OP width (mm)	ES enhancement*	Time from onset to MRI (days)
1	57, M	R	105/47	Flat	No	0.7	1.3	2	12
2	53, F	L	80/67	Flat	No	0.5	0.8	2	28
3	25, M	L	46/0	Flat	No	0.7	0.9	2	2
4	55, M	R	113/103	Flat	No	0.9	1.4	2	6
5	25, F	R	85/52	Flat	No	0.3	0.6	2	8
6	22, M	L	80/17	Up-sloping	Yes	0.8	1.3	1	13
7	56, M	R	78/30	Flat	No	0.5	1.4	2	48
8	62, M	L	80/72	Up-sloping	No	0.6	1.1	1	3
9	52, F	L	68/13	Flat	No	0.6	1.1	2	8
10	57, M	R	87/15	Up-sloping	No	0.8	1.2	0	2
11	51, M	R	100/75	Flat	No	0.6	1.2	1	8
12	59, M	R	97/28	Up-sloping	No	0.5	0.9	0	6
13	64, M	R	95/80	Flat	Yes	0.4	0.5	2	18
14	79, F	R	83/67	Down-sloping	Yes	0.6	0.8	2	8
15	56, M	R	77/57	Flat	No	0.6	0.8	1	13
16	51, F	L	93/25	Flat	No	0.7	1	1	4
17	62, M	L	78/78	Up-sloping	No	0.5	0.7	2	20
18	50, F	R	115/108	Flat	No	0.8	1.3	2	2
19	70, F	L	102/90	Flat	Yes	0.8	0.9	2	14

*Hearing level was expressed as the average score at three frequencies (500, 1000 and 2000 Hz), for the initial and final audiogram. †0 = no enhancement; 1 = ipsilateral enhancement; 2 = bilateral enhancement. Yr = years; MP = vestibular aqueduct at midpoint; OP = vestibular aqueduct at operculum; ES = endolymphatic sac; MRI = magnetic resonance imaging; M = male; F = female; R = right; L = left

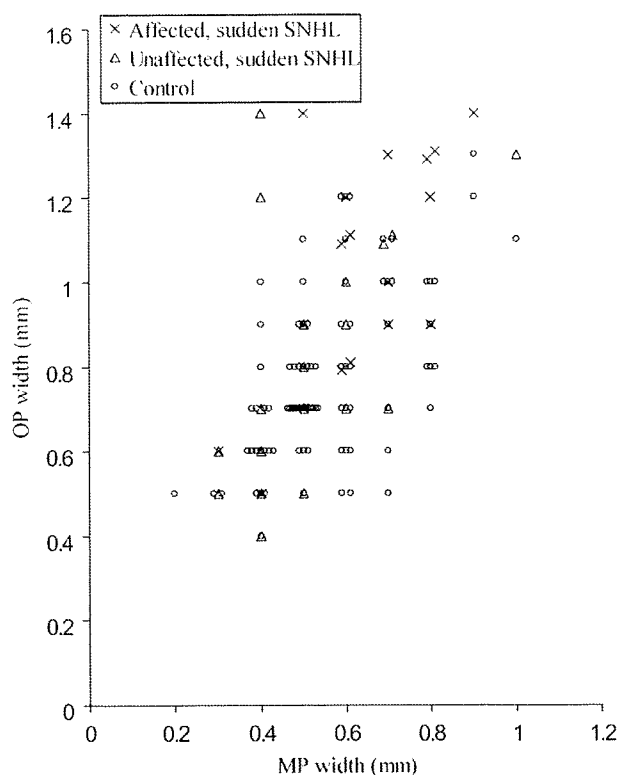


FIG. 2

Scatter plot of vestibular aqueduct widths at the operculum versus those at the midpoint, in affected and unaffected ears of patients with sudden sensorineural hearing loss and in control subjects. MP = midpoint; OP = operculum; SNHL = sensorineural hearing loss

enhancement of the endolymphatic sac did not differ significantly, comparing those patients examined with 1.5-Tesla MRI and those examined with 3-Tesla MRI.

Enhancement of the endolymphatic sac was judged to be present on the affected side in 17 patients (89 per cent). In 11 of these 17 patients, the enhancement was also judged to be present on the contralateral side. However, no enhancement was observed on the contralateral side only.

The frequency of enhancement of the endolymphatic sac was significantly greater in the SNHL-affected ears than in the contralateral ears ($p < 0.05$). In patients with sudden SNHL, the period between the onset of hearing loss and MRI scanning did not differ significantly between those patients who showed enhancement (average \pm SD, 12.6 ± 11.4 days) and those who did not (4.0 ± 2.8 days).

In patients with sudden SNHL, the width of the vestibular aqueduct at the midpoint and operculum in the SNHL-affected ear did not differ significantly, comparing patients with enhancement of the endolymphatic sac (midpoint, 0.6 ± 0.2 mm; operculum, 1.0 ± 0.3 mm) and those without enhancement (midpoint, 0.7 ± 0.2 mm; operculum, 1.1 ± 0.2 mm). Furthermore, no difference in prognosis scores was noted between sudden SNHL patients with and without enhancement.

Discussion

The major finding of this study was that the width of the vestibular aqueduct in the ear affected with sudden SNHL was significantly greater than that in the contralateral ear or in the ears of control subjects. It has been reported that the width of the vestibular aqueduct is smaller in patients with Ménière's disease than in control subjects.^{6,7} Evaluation of the vestibular aqueduct is important to our understanding of the pathophysiological mechanisms involved in sudden SNHL, considering that the vestibular aqueduct size in patients with sudden SNHL differs from that in patients with Ménière's disease.

Enlarged vestibular aqueduct is the most common congenital abnormality in the inner ear on radiological assessment. Enlarged vestibular aqueducts have been associated with a range of congenital disorders, such as the CHARGE association was defined as a non-random association of anomalies (Coloboma, Heart defect, Atresia choanae, Retarded growth and development, Genital hypoplasia, Ear anomalies/deafness), association,¹⁵ Alagille syndrome,¹⁶ Pendred syndrome¹⁷ and the branchio-oto-renal syndrome.¹⁸ The criteria to determine an enlarged vestibular aqueduct are vague. However, a vestibular aqueduct diameter larger than 1.5 mm at the midpoint or an opercular measurement of greater than 2 mm are generally considered to be the defining characteristics.^{19,20} In the present study, all patients with sudden SNHL showed a vestibular aqueduct diameter of less than 1.5 mm at the midpoint or an opercular measurement of less than 2 mm. Thus, we found that none of the patients in this study showed evidence of an enlarged vestibular aqueduct.

Purcell *et al.*²¹ reported significant differences in the shape of the inner ear in patients with congenital SNHL, even in cases with grossly normal CT scans, when compared in detail with those of patients without SNHL. These authors suggested that hearing loss in SNHL patients with a 'radiologically normal' cochlea may be related to dysfunction of both the membranous and bony labyrinths. However, they did not evaluate the vestibular aqueduct quantitatively.

- This study sought to evaluate the vestibular aqueduct in patients with sudden sensorineural hearing loss
- Nineteen patients with sudden SNHL were evaluated using computed tomography and magnetic resonance imaging
- The width of the vestibular aqueduct in SNHL-affected ears at the midpoint and operculum was significantly greater than that in contralateral, unaffected ears or in control ears
- It is possible that sudden SNHL patients with a wider vestibular aqueduct are born with a 'fragile' inner ear
- Clarifying the pathophysiological mechanism responsible for endolymphatic sac enhancement may aid the understanding of sudden deafness

Our previous study demonstrated that the endolymphatic sac was enhanced in 75 per cent of sudden SNHL-affected ears, in 53 per cent of contralateral ears in patients with sudden SNHL and in 18 per cent of control ears.⁸ In the present study, the endolymphatic sac was enhanced in 89 per cent of sudden SNHL ears and in 63 per cent of the contralateral ears of patients with sudden SNHL. The frequency of endolymphatic sac enhancement in patients with sudden SNHL did not differ significantly between the previous and the present study (chi-square test). Enhancement of the endolymphatic sac suggests inflammation of the endolymphatic sac tissue or venous enlargement in the region of the sac. Based on the results of this study, we speculate that many patients with sudden SNHL may experience pathophysiological changes in the region of the endolymphatic sac. We have previously reported that the endolymphatic sac was enhanced in 63 per cent of affected ears in patients with acute low-tone SNHL without vertigo.²² In contrast, the endolymphatic sac was enhanced in 20 per cent of affected ears in patients with Ménière's disease.⁸

It is known that the endolymphatic sac and duct are poorly developed in patients with Ménière's disease. The endolymphatic sac is believed to intervene in the absorption of the endolymphatic fluid, and damage to the endolymphatic sac results in endolymphatic hydrops.²² It is possible that the narrow vestibular aqueduct in patients with Ménière's disease is associated with an impediment of the absorption of endolymphatic fluid. In contrast, the results of the present study show that the vestibular aqueduct in patients with sudden SNHL was wider than that in controls. A wider vestibular aqueduct might be associated with insufficient maturation of the inner ear, because an increased fluid-filled area of the inner ear may be related to insufficient maturation of the inner ear.²³ It is possible that sudden SNHL patients with a wider vestibular aqueduct are born with a 'fragile' inner ear,⁴ or are apt to receive abnormal pressure transmission through the vestibular aqueduct.²⁴

Clarifying the pathophysiological mechanism responsible for endolymphatic sac enhancement in patients with sudden deafness may be a key to understanding the cause of sudden deafness. Precise imaging and evaluation of the inner ear is essential to the investigation of the pathological conditions underlying sudden SNHL.

References

- Fitzgerald DC, Mark AS. Sudden hearing loss: frequency of abnormal findings on contrast-enhanced MR studies. *AJNR Am J Neuroradiol* 1998;**19**:1433-6
- Okamoto M, Shitara T, Nakayama M, Takamiya H, Nishiyama K, Ono Y *et al*. Sudden deafness accompanied by asymptomatic mumps. *Acta Otolaryngol (Stockh)* 1994;**514**:45-8
- Shinohara S, Yamamoto E, Saiwai S, Tsuji J, Muneta Y, Tanabe M *et al*. Clinical features of sudden hearing loss associated with a high signal in the labyrinth on unenhanced T1-weighted magnetic resonance imaging. *Eur Arch Otorhinolaryngol* 2000;**257**:480-4
- Sugiura M, Nakashima T, Naganawa S, Otake Y, Mukaida T, Sone M *et al*. Sudden sensorineural hearing loss associated with inner ear anomaly. *Otol Neurotol* 2005;**26**:241-6
- Nakashima T, Naganawa S, Sone M, Tominaga M, Hayashi H, Yamamoto H *et al*. Disorders of cochlea blood flow. *Brain Res Rev* 2003;**43**:17-28
- Sando I, Orita Y, Hirsch BE. Pathology and pathophysiology of Meniere's disease. *Otolaryngol Clin North Am* 2002;**35**:517-28
- Krombach GA, van den Boom M, Di Martino E, Schmitz-Rode T, Westhofen M, Prescher A *et al*. Computed tomography of the inner ear: size of anatomical structures in the normal temporal bone and in the temporal bone of patients with Meniere's disease. *Eur Radiol* 2005;**15**:1505-13
- Naganawa S, Koshikawa T, Fukatsu H, Ishigaki T, Nakashima T, Ichinose N. Contrast-enhanced MR imaging of the endolymphatic sac in patients with sudden hearing loss. *Eur Radiol* 2002;**12**:1121-6
- Nakashima T, Kuno K, Yanagita N. Evaluation of prostaglandin E1 therapy for sudden deafness. *Laryngoscope* 1989;**99**:542-6
- Naganawa S, Itoh T, Fukatsu H, Ishigaki T, Nakashima T, Ichinose N *et al*. MR imaging of the inner ear: comparison of three-dimensional fast spin-echo sequence with use of a dedicated quadrature-surface coil with a gadolinium-enhanced spoiled gradient-recalled sequence. *Radiology* 1998;**208**:679-85
- Naganawa S, Itoh T, Fukatsu H, Ishigaki T, Nakashima T, Kassai Y *et al*. Three-dimensional fast spin-echo MR of the inner ear: ultra-long echo train length and half-fourier technique. *AJNR Am J Neuroradiol* 1998;**19**:739-41
- Sugiura M, Naganawa S, Teranishi M, Nakashima T. Three-dimensional fluid-attenuated inversion recovery magnetic resonance imaging findings in patients with sudden sensorineural hearing loss. *Laryngoscope* 2006;**116**:1451-4
- Kawase S, Naganawa S, Sone M, Ikeda M, Ishigaki T. Relationship between CT densitometry with a slice thickness of 0.5 mm and audiometry in otosclerosis. *Eur Radiol* 2006;**16**:1367-73
- Madden C, Halsted M, Benton C, Greinwald J, Choo D. Enlarged vestibular aqueduct syndrome in the pediatric population. *Otol Neurotol* 2003;**24**:625-32
- Murofushi T, Ouvrier RA, Parker GD, Graham RI, da Silva M, Halmaqvi GM. Vestibular abnormalities in CHARGE association. *Ann Otol Rhinol Laryngol* 1997;**106**:129-34
- Okuno T, Takahashi H, Shibahara Y, Hashida Y, Sando I. Temporal bone histopathologic findings in Alagille's syndrome. *Arch Otolaryngol Head Neck Surg* 1990;**116**:217-20
- Phelps PD, Coffey RA, Trembath RC, Luxon LM, Grossman AB, Britton KE *et al*. Radiological malformations of the ear in Pendred syndrome. *Clin Radiol* 1998;**53**:268-73
- Chen A, Francis M, Ni L, Cremers CW, Kimberling WJ, Sato Y *et al*. Phenotypic manifestations of branchio-oto-renal syndrome. *Am J Med Genet* 1995;**58**:365-70
- Valvassori GE, Clemis JD. The large vestibular aqueduct syndrome. *Laryngoscope* 1978;**88**:723-8
- Levenson MJ, Parisier SC, Jacobs M, Edelstein DR. The large vestibular aqueduct syndrome in children. A review of 12 cases and the description of a new clinical entity. *Arch Otolaryngol Head Neck Surg* 1989;**115**:54-8
- Purcell DD, Fischbein N, Lalwani AK. Identification of previously "undetectable" abnormalities of the bony labyrinth with computed tomography measurement. *Laryngoscope* 2003;**113**:1908-11
- Sugiura M, Naganawa S, Nakashima T, Misawa H, Nakamura T. Magnetic resonance imaging of endolymphatic sac in acute low-tone sensorineural hearing loss without vertigo. *ORL J Otorhinolaryngol Relat Spec* 2003;**65**:254-60
- Ishida IM, Sugiura M, Naganawa S, Teranishi M, Nakashima T. Cochlear modiulus and lateral semicircular canal in sudden deafness. *Acta Otolaryngol* 2007; 1-5 (Epub ahead of print)

24 Boston M, Halsted M, Meizen-Derr J, Bean J, Vijayasekaran S, Arjmand E *et al.* The large vestibular aqueduct: a new definition based on audiologic and computed tomography correlation. *Otolaryngol Head Neck Surg* 2007;**136**:972-7

Address for correspondence:
Dr Makoto Sugiura,
Department of Otorhinolaryngology,
Nagoya University Graduate School of Medicine,

65 Tsurumai-cho, Showa-ku,
Nagoya 466-8550, Japan.

Fax: +81 52 744 2325
E-mail: makotos@med.nagoya-u.ac.jp

Dr M Sugiura takes responsibility for the integrity of the
content of the paper.

Competing interests: None declared
